AN AUTOMATIC IMAGE ANALYSIS APPROACH TO QUANTIFY STAINED CELL CULTURES

E. GLORY [1,2,3], G. DEROCLE[3], N. OLLIVIER[3], V. MEAS-YEDID[1],
G. STAMON[2], C. PINSET[3] AND J-C. OLIVO-MARIN[1]

[1] Laboratoire d'Analyse d'Images Quantitative, Institut Pasteur, 25 rue du Dr Roux, 75015 Paris, France
[2] Laboratoire des Systèmes Intelligents de Perception-CRIP5, Université Paris 5, 45 rue des Saints-Pères,
75006 Paris, France
[3] Celogos, 4 rue Pierre Fontaine, 91 058 Evry Cedex, France
Fax: +33 1 40 61 33 30, Email: glory@math-info.univ-paris5.fr, vmeasyed@pasteur.fr

Abstract – Counting cells in culture is a common task in biotechnology research and production. This process should be automated to provide fast and objective quantification. Flow cytometry is adapted to count cells in suspension. However, the morphological information and the spatial organisation of adherent cells are lost when cells are removed from culture. This paper proposes a methodology based on image analysis to quantify stained nuclei in culture. The protocol is composed of several steps: cell staining, automatic microscopy imaging, segmentation by an automatic algorithm including a classification approach, and computation of quantitative data that characterizes the growth of cells. An evaluation shows that the automatic process of counting provides results similar to human manual counting. The major interests of the proposed approach are the fully automated processing and preservation of cell shapes and positions in culture. More than two thousand culture conditions have been measured by this tool for various applications including optimization of cell culture media, improvement of the culture processes and measurement of drug toxicity.

Key words: colour image analysis, cytology, stained cell cultures, automatic segmentation, nonparametric classification, splitting aggregated nuclei

INTRODUCTION

Cell culture is widely used in research and production laboratories to study cell properties and the influence of the environment. A manual evaluation of the cultures is tedious, time consuming and yields subjective results. For this reason, automated solutions have been designed to produce quantitative and objective data. Flow cytometry is the usual device employed to count and sort cells in suspension. However, this approach is not completely satisfying to study adherent cells because the morphological features and the spatial organization are lost when cells are detached from the culture surface. Quantitative image analysis is an interesting alternative to extract these characteristics.

Owing to improvements in microscopy, the increasing quality of digital cameras and the higher capacity of computers, the use of biological images has increased over the last ten years. Many algorithms have been developed and adapted to automatically segment biological images. Image segmentation refers to the partition of an image into a set of regions with specific properties. In a segmented image, the elementary picture elements are no longer the pixels but connected sets of pixels (11). Once the image has been segmented, measurements are performed on each region and adjoining relationships between regions can be investigated. Image segmentation is therefore a key step towards the quantitative interpretation of image data. To design an algorithm which segments an image into meaningful regions, some prior knowledge about the image (noise, magnification, contents…) and the objects of interest (object number, shape, size, orientation, grey level distribution, color, texture…) are required. Ideally, region features should allow the discrimination of different objects in the image. Unfortunately, features enabling the recognition of all image objects are seldom available in practical applications. As a consequence, no general algorithm exists to produce optimal segmentations for all images (14). Several papers deal with the segmentation of cells: approaches are histogram-based thresholding, edge detection (4), multi-spectral analysis (2,9), morphological mathematics and skeletonization (1,5), region growing (21), classification (12), parametric active contours (3,22) or level sets (8,20). Other methods have been proposed to separate aggregated cells, requiring the cell edge profile (3), the shape of cells (7) or the modeling of cells (6). Our application is focused on nuclei which are smaller, more numerous and aggregated objects compared to cells studied in the previous

solutions. Unfortunately, existing methods are not suitable to treat these characteristics. Microscopy images are taken with a low magnification to observe the largest field of cells in which nuclei are distinguishable. Here we present a fully automated method developed to classify and segment small aggregated nuclei.

This paper proposes a method to automatically analyze *in vitro* cell cultures by image analysis. Different parts of the methodology are reported, such as cell culture preparation, microscopy image acquisition, image segmentation to find objects of interest, classification step and computation of descriptive data.

Among the applications that motivated the project, is our interest in characterizing the growth of cells in culture. The chosen approach aims to analyze adherent cells in multi-well plates by studying their nuclei. We consider cell types which have only one nucleus per cell. This includes immature muscular cells and bone marrow cells. Thus, the number of cells is directly deduced from the number of nuclei. To avoid practical constraints such as a culture chamber adapted to the microscope, cell cultures are fixed, stained and observed with a brightfield microscope. The Giemsa dye is used to stain nuclear structures in magenta. However, this dye occasionally colors the cytoplasm of cells. The coloration is homogeneous inside a well but slight variations are present from one well to another, depending on the differentiation stage and the density of cells.

MATERIALS AND METHODS

Cell culture

Adherent cells used in the studied experiments are immature muscular cells and bone marrow cells of human or animal (rat, sheep) origin. Cells are cultured in 12, 24 or 96 multi-well plates in standard conditions of growth (5% CO_2, 37°C). The composition of culture media differs among experiments, and each experiment is performed at least in triplicate.

Cell preparation

To analyze a multi-well plate, the culture medium is removed and cells are rinsed with PBS 1X. Samples are fixed by immersion in ethanol for 10 min. After rinsing with water, cells are stained with 1 ml of Giemsa dye diluted 1:10 during 5 to 10 min. Plates are re-rinsed with water. As a consequence, the stain is stable (see figure 1) and plates can be stored in a dry place for several months.
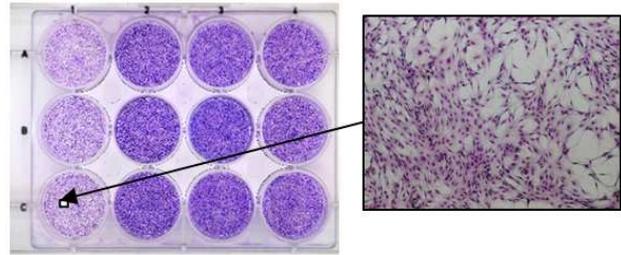

Figure 1. Illustration of a 12-multiwell plate where experiments are performed in triplicate. On the right, we show an image taken with a 10x objective.

Microscopy image acquisition

The acquisition system is composed of an inverted motorized microscope (TE-2000E, Nikon), a CDD color camera (DXM1200F, Nikon) and the software which controls the position of the plate stage, the autofocus, the acquisition and the storage of images (Lucia, Laboratory Imaging Ltd). The parameters of magnification (10x), color balance, luminosity (6V), time exposure (6 ms), filters and calibration are identical for all the experiments. Thanks to scripts adapted to the different plates, the acquisition procedure is fully automatic. The system acquires about 300 images per hour. The color images are sized 716*976 pixels, and saved in 24 bit TIFF format. A single well of a 12-multiwell plate contains 300 inclusive images, we empirically evaluated that the error rate of nuclei counting is less than 10% when it is estimated with 50 images only. Thus, in most of the experiments the difference between conditions are enough to be visible by taking 50 images per well.

Image Analysis

The algorithms developed in this project are written in Java and integrated into the ImageJ software (15) to be run on all platforms. ImageJ is an open-source software developed by Wayne Rasband of the National Institute of Health (U.S.A). It is mostly used by biologists but not limited in its applications. In this project, an interface was designed to allow users to specify experiment-dependent information such as the plate identification, the number of images per well, the number of wells per condition, the type of cells, the culture medium, the number of seeded cells and the number of days in culture. The descriptive data computed by the algorithm are stored in an Excel file and segmented images are displayable to check the segmentation results.

Computation of cell growth features

In order to interpret and to compare the experiments, the recovery rate and the doubling time are systematically computed. The computation of this information requires seeding as many identical multiwell plates at the first day (day 0) as the time points necessary to compute these data. 24 hours after the seeding, one plate is fixed, stained, and nuclei are quantified by image analysis, to count the number of adherent cells before cell divisions (day 1). The recovery rate measures the capacity of cells to adhere to the plate, since cells which are not attached to the plate, for different reasons, are eliminated by the rinsing steps:

$$recovery\ rate\ =\ \frac{number\ of\ cells\ at\ Day\ 1}{number\ of\ cells\ at\ Day\ 0}$$

Other plates are fixed later to measure the growth of cells for different culture times. If we assume that the growth of cells follows an exponential law, and n_2 and n_3 are the number of cells counted on Day 2 and Day 3, respectively, then the doubling time t is computed as follows:

$$ t = \frac{\log\left(\dfrac{n_3}{n_2}\right)}{\log(2)} $$

IMAGE ANALYSIS APPROACH

Color segmentation

The goal of the segmentation is to subdivide an image into regions from which objects of interest are distinguished from the background. The global strategy is to define a fast and robust algorithm to treat a great quantity of images. We have chosen to reduce color images into gray level images and to apply an automatic threshold on the histogram (16).

There are several ways to reduce the 3-dimensionnal color information into 1-dimension values. The intuitive approach consists in choosing the color component which produces the best segmentations. In this case, a *color component* represents only one axis among the three axes which encode the color information. This is achieved automatically by using a quantitative criterion C, designed to measure the quality of color segmentations of cytological images (10,13). This criterion includes two normalized terms which penalize color heterogeneity of segmented regions and the number of small regions:

$$ C(I) = \frac{\sum\limits_{i=1}^{R} \dfrac{e_i^2}{1+\log(A_i)}}{1+\dfrac{e^2}{1+\log(A)}} + \frac{\sum\limits_{j=A_{\min}}^{A_{\max}} \dfrac{R(A_j)}{A_j^2}}{R} $$

where I is the segmented image, A the size of the image, R the number of segmented regions and e the average color heterogeneity of the image. A_i and e_i are respectively, the area and the average color heterogeneity of ith region. e_i^2 is defined as the sum of the Euclidean distances between the original image and the mean color of the segmented region, evaluated for each pixel p belonging to region i, and computed in a uniform color space such as Lu*v*:

$$ e_i^2 = \sum_{p \in i}\left(L_p - \overline{L_i}\right)^2 + \left(u^*_p - \overline{u^*_i}\right)^2 + \left(v^*_p - \overline{v^*_i}\right)^2 $$

$R(A_i)$ represents the number of regions with an area equal to A_i. The first term penalizes regions with high color heterogeneity, while the second term penalizes noisy regions of small size. With this criterion, a good segmentation is a trade-off between the color homogeneity and the absence of small regions.

Various color spaces have been tested: RGB, normalized rgb, Lu*v*, La*b*, YUV, YIQ, I1I2I3, H1H2H3, HSB, XYZ and opponent colors. The normalized rgb color space is robust to variations of illumination because $r=R/I$, $g=G/I$, $b=B/I$ with $I=R+G+B$. For each color component from each color space, the segmentation is performed with the automatic threshold of Ridler (16). From trials on 25 sample images, we found that the green component of the normalized rgb color space, g, provides on average the lowest C value, implying that g produces the best segmentations (see figure 2). On our images, the g component is enough to produce segmentations with a good quality; otherwise we would combine the components which provide the lowest C values to improve the segmentation.
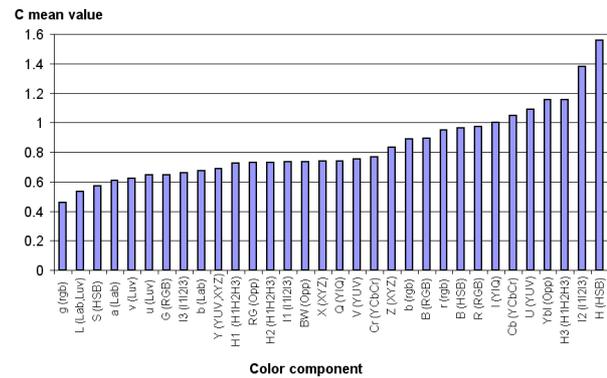

Figure 2. Comparison of the segmentation quality as function of the color component used for automated threshold.
Smaller mean C values indicate better segmentations. All color spaces are not showed here.

This result is confirmed by a principal component analysis of the normalized rgb color space (see figure 3), and concurs with the practice of biologists who have observed the green channel when they study Giemsa stained samples.
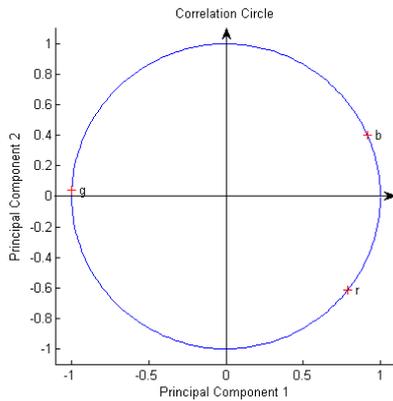
46

Figure 3. The correlation circle shows a projection of the initial variables (r,g,b) in the factors space.
95.6 % of the variability is explained by the first principal component and 98.7% by considering the two first axes. The first axis is positively correlated to the blue and red variables but strongly negatively correlated to the green variable. Thus, the green variable contains almost all the information of the initial color.

The interest of this approach, based on the criterion C, is to select the conditions which produce the best segmentation among the methods and the parameter values tested.

As a second step, we apply a morphological opening to eliminate isolated pixels and smooth region edges. The binary images distinguish nuclei and background (see figure 4). For various reasons -cell origins, differentiation stage or density- nuclei aggregate. In order to provide an accurate quantification and a precise study of the culture, aggregated nuclei must be split. To identify them, a classification method is carried out to distinguish isolated and aggregated nuclei. Next, a split and merge algorithm is applied to the class of aggregated nuclei to find the frontier of individual nuclei.
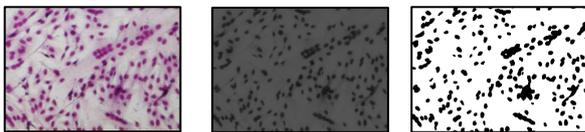

Figure 4. The color image is reduced into gray level by taking the green component of the normalized RGB color space.
Then, Ridler's automatic threshold produces a binary image where background and stained nuclei are distinguished.

Classification

The classification is based on the morphology of the connected components. The size is not sufficient for the classification because some of the aggregates are smaller than isolated nuclei. We have considered more features, including area, perimeter, major and minor axes of the best fitted ellipse, elongation and circularity. Their undefined distributions and the variability of values among experiments make impossible the determination of fixed range to define classes. Moreover supervised learning by labeling samples is not conceivable in an automated process. Consequently, we chose a nonparametric method to estimate the probability density of the prototypes corresponding to the connected components projected in the feature space (18). Features are normalized between 0 and 1, and the probability density $p(X_0)$ of a prototype X_0 is computed as follows:

$$p(X_0) = \frac{1}{n} \sum_{i=1}^{n} \frac{1}{h^d} \varphi\left(\frac{X_0 - X_i}{h}\right)$$

where n is the number of prototypes, h^d is the window length of the d-dimension hypercube. In this case, d=6 because we use 6 features to describe each prototype. φ is the Parzen kernel defined as:

$$\varphi(X) = \begin{cases} 1 & \text{if } |X_j| < 1/2 \,; \ j = 1,...,d \\ 0 & \text{else} \end{cases}$$

Assuming that the majority of the connected components corresponds to individual nuclei and shares similar features, as it is the case in the experiments that we considered, the Parzen window calculates a high density around their characteristics, while the connected components with a low density are attributed to the aggregate class. The two parameters of this approach have been determined empirically: the length of the window h was set to *0.1* and a frontier between the prototypes classified as isolated and aggregated defined at 20% of the maximum probability density. In this manner, the features of isolated prototypes are automatically learned with a training set of about thousand nuclei from each experiment. Subsequently, the connected components of the images coming from the same experiment are classified according to the value of the density probability computed on the individual nuclei identifyed in the training set. The rate of false negatives (the number of true aggregates classified as isolated nuclei) is less than 4% and the rate of false positives (the

number of true isolated nuclei classified as aggregates) is less than 12%. This classification method thus provides a class of connected components largely composed of aggregates. The next processing step deals with the class of aggregates in order to split them into individual nuclei.

Split and Merge

The proposed strategy to extract individual nuclei from aggregates is composed of two steps. The first step splits the connected component into regions with features similar to those of isolated nuclei. Because this step produces an over-segmentation, some of the regions are merged in a second step.

For splitting the connected components of the aggregate class, we chose a watershed algorithm applied either on the green component image, or on the distance map computed from the binary image. The watershed algorithm (19) simulates the flooding of catchment basins with water (see figure 5).
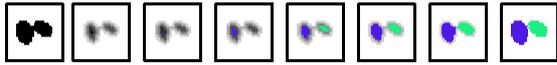
Figure 5. Watershed algorithm evolution on the distance map (2nd image) of a binary object (1st image).
Gray levels are flooded from darker to brighter. A dam is built when two catchment basins strike.

The probability density of each region is computed and only the region with the highest value is retained. The other regions are merged together and this process is applied iteratively until the last region can no longer be divided. Then, all partition combinations are computed and the combination that produces the minimum cost function is chosen. The cost function *f*, called *merging function*, compares the area of each region A_i with the area of a standard isolated nucleus A_{ref}. The latter is found from the features of the connected component which has the highest value of the probability density in the classification training step. The merging function also takes into account the variability of the area between the regions that compose the partition by including the standard deviation of the area σ_A:

$$f = \frac{\sum_{i=1}^{k}\left|A_i - A_{ref}\right|}{k} + \sigma_A$$

This algorithm splits the aggregates into regions that share the features of individual nuclei (see figure 6).
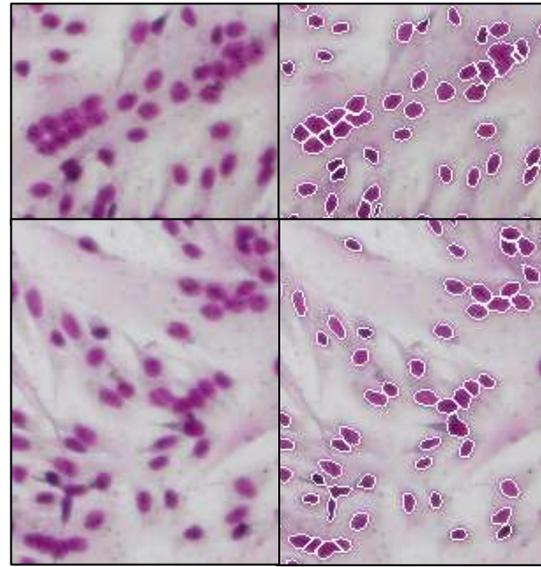
Figure 6. Crop pictures from original images (on the left) and their segmentations (on the right).
White lines surround segmented regions.

Data Analysis

Once segmentation is achieved, different measurements can be computed on nuclear regions in order to characterize their position, shape, size and color. Accurate segmentation of nuclei is important to determine the growth of cells, such as the recovery rate and the doubling time (see Material and Method section). Moreover, the density and the morphology of nuclei allow biologists to interpret the evolution of cell growth and differentiation.

RESULTS AND DISCUSSION

The proposed method of segmentation has been validated by comparing the number of nuclei manually counted and the quantitifcation by the automated process. Table A reports the results obtained on two muscular cell cultures and one bone marrow cell culture.

The error in counting is about 1 to 7% for aggregated nuclei while it is negligibly small for isolated nuclei (0.02 to 0.4%). Since there are more isolated nuclei than aggregated nuclei, the total rate of errors is less than 2%. Thus, the number of nuclei counted with this algorithm is similar to those counted by humans on non-confluent cultures. Thus this tool can be reliably used to quantify nuclear characteritics of adherent cells.

Table 1. Comparison of nuclei counting by a human (manual counting) and by the proposed algorithm. The rate of error is about 1%.

	Number of nuclei (manual)	Number of nuclei (automatic)	Error rate
Muscle cells A	7 357	7 318	0.53 %
Muscle cells B	5 072	5 038	0.67 %
Bone marrow cells	7 065	6 940	1.77 %
Total	**12 905**	**12 885**	**1.01 %**

This algorithm has already been used to study more than 200,000 photos, representing about 2,000 culture conditions. Applications of the proposed protocol are numerous. We used it to complete studies of the toxicity of different statins on muscular cells, to optimize the growth of muscular cells extracted from a human biopsy (see figure 6), to improve the freezing protocol from measures of cell recovery rate and to control the quality of cell proliferation in a therapeutic protocol of urinary incontinence.
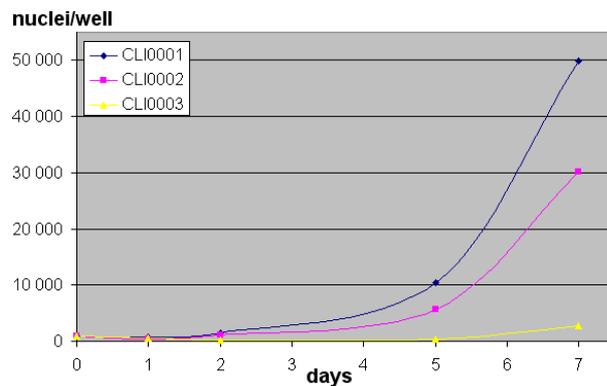

Figure 7. Growth of muscular cells in culture coming from different biopsies.
The automatic algorithm has computed the number of cells cultured for various times.

These encouraging results obtained with the proposed cell counting methodology allow the study of other cellular features, such as the organization of nuclei during the differentiation stage. Another interest to biologists is the ability to quantitatively study the distribution of nuclear size, which can be informative about a cell's capacity to divide.

The distinction of isolated nuclei and aggregates might be seen as as a *one class classification* problem (17) because only features of isolated nuclei are well defined. Aggregates can have various shape. We plan to study this approach in a future.

CONCLUSION

We have described a computerized image analysis system developed to automatically quantify stained cell cultures. To assess the capacity of a given medium to favor cell growth, we measured the increase in the number of nuclei at given intervals. Nuclei segmentation is achieved by thresholding the normalised green component of color images. The choice of the green color component was based on a quantitative assessment of the segmentation quality thanks to a newly proposed criterion. The nuclei segmentation was improved by using an automatically trained classification method that determines the isolated nuclei features in each experiment. Aggregated nuclei are split into individual nuclei by a supervised split and merge approach using the previously determined isolated isolated nuclei features. Our results show that the number of nuclei counted with this algorithm is similar to human counting with a rate of error less than 2% in non-confluent cultures. The presented image analysis tool is routinely used in a number of applications, including quality control and drug toxicity tests. Future work will address the study of muscular fibers by quantifying the nuclei spatial relationships and their link to tissue function.

REFERENCES

1. Angulo, J. and Flandrin, G., Automated detection of working area of peripheral blood smears using mathematical morphology. *Analytical Cellular Pathology*, 2003, **25-1**:37-49.
2. Aggarwal, R.K. and Bacus, J.W., A multi-spectral approach for scene analysis of cervical cytology smears, *Journal of Histochemistry and Cytochemistry*, 1977, **25-7**:668-680.
3. Bamford, P., In: *Segmentation of cell images with an application to cervical cancer screening*. PhD thesis - University of Queenland, 1999.
4. Brenner, J.J., Necheles, T.F., Bonacossa, I.A., Necheles, T.F., Fristensky, R., Weintraub, B.A. and Neurath, P.W.,

Scene segmentation techniques for the analysis of routine bone marrow smears from acute lymphoblastic leukaemia patients. *Journal of Histochemistry and Cytochemistry*, 1977, **25-7**: 601-613.

5. Cloppet, F., Oliva, J.M and Stamon, G., Angular Bisector Network, a Simplified Generalized Voronoï Diagram: Application to Processing Complex Intersections in Biomedical Images. *IEEE Trans. on Pattern Analysis and Machine Intelligence*, 2000*,* **22-1**: 120128.

6. Cong, G. and Parvin, B., Model-based segmentation of nuclei, *Pattern Recognition*, 2000, **33**: 1383-1393.

7. Delingette, H. and Montagnat, J., Shape and Topology Constraints on Parametric Active Contours, *Computer Vision and Image Understanding*, 2001, **83-2**: 359-369.

8. Dufour, A., Shinin, V., Tajbakhsh, S., Guillen-Aghion, N., Olivo-Marin, J.-C. and Zimmer, C., Segmenting and Tracking Fluorescent Cells in Dynamic 3-D Microscopy with Coupled Active Surfaces, *IEEE Trans. on Image Processing*, 2005, **14-9**: 1396-1410.

9. Fernandez, G., Kunt, M. and Zryd, J.-P., Multi-spectral based cell segmentation and analysis. *Proc. of the Workshop on Physics-based Modelling in Computer Vision*, Cambridge, USA, 1995, 166-172.

10. Glory, E., Meas-Yedid, V., Pinset, C., Olivo-Marin, J-C. and Stamon, G., A Quantitative Criterion to Evaluate Color Segmentations. Application to Cytological Images, In: *Lecture Notes in Computer Science*, Springer-Verlag GmbH, 2005, **3708**:227-234.

11. Gonzalez, R.C. and Wintz, P., *Digital Image Processing.* Addison Wesley, 1987, 122-125.

12. Lebrun, G., Charrier, C., Lezoray, O., Meurie, C and Cardot, H.: Fast Pixel Classification by SVM Using Vector Quantization, Tabu Search and Hybrid Color Space. *CAIP*, 2005, 685-692.

13. Meas-Yedid, V., Glory, E., Morelon, E., Pinset C. and Olivo-Marin, J.-C. Automatic color space selection for biological image segmentation. *International Conference of Pattern Recognition* , 2004, **3**:514-517.

14. Pal, N. R. and Pal, S. K., A review on image segmentation techniques. *Pattern Recognition*, 1993, **26-9**: 1277-1294.

15. Rasband, W., ImageJ Version 1.31s. *http://rsb.info.nih.gov/ij/,* National Institutes of Health, USA, 2005.

16. Ridler, T.W. and Calvard Clarke, S., Picture thresholding using an iterative selection method. *IEEE Trans. System, Man and Cybernetics*, 1978, **8**: 630-632.

17. Schölkopf, B., Platt, J., Shawe-Taylor, J., Smola, A. J. and Williamson, R. C., Estimating the support of a high-dimensional distribution. *Neural Computation*, 2001, **13**:1443-1471.

18. Theodoridis, S. and Koutroumbas, K., *Pattern Recognition*. Accademic Press, 1999, 13-20.

19. Vincent, L. and Soille, P., Watersheds in digital spaces: an efficient algorithm based on immersion simulations. *IEEE Trans. on Pattern Analysis and Machine Intelligence*, 1991, **13-6**: 583-598.

20. Xie, X. and Mirmehdi, M., Level-set based geometric color snakes with region support. *Proc. of International Conference on Image Processing*, 2003, **2**: 153-156.

21. Zhang, X.-W., Song, J.Q., Lyu, M. R. and Cai, S.J., Extraction of karyocytes and their components from microscopic bone marrow images based on regional color features. *Pattern Recognition*, 37:351-361, 2004.

22. Zimmer, C., Labruyère, E., Meas-Yedid, V., Guillèn, N. and Olivo-Marin, J.-C., Segmentation and Tracking of Migrating Cells in Videomicroscopy with Parametric Active Contours: a Tool for Cell-Based Drug Testing. *IEEE Trans. Med. Imaging,* **21-10**:1212-1221, 2002.